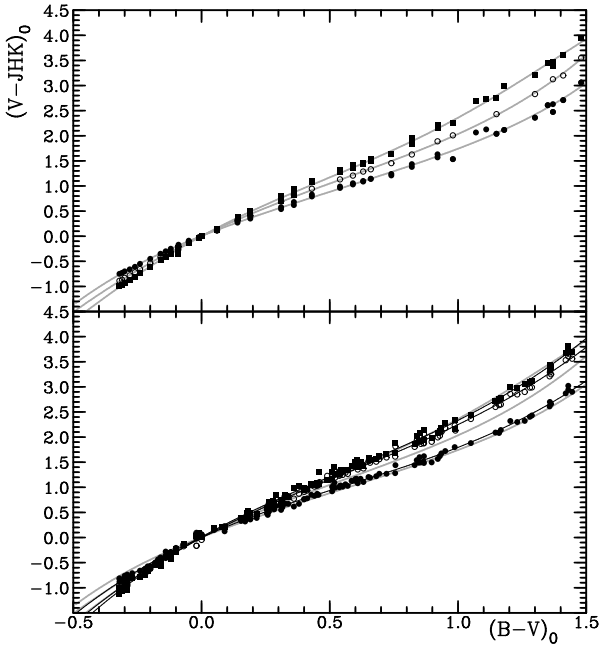

Fig. 1. Intrinsic $(V–K)_0$ (filled squares), $(V–H)_0$ (open circles), and $(V–J)_0$ (filled circles) colors for main-sequence stars are plotted as functions of intrinsic $(B–V)_0$ color from Johnson (1968) and Koornneef (1983) in the upper portion of the diagram. The adopted relations from least squares fits are denoted by gray curves. The lower diagram plots observed data for photometric standards and standard stars using the same symbols as above. Solid curves denote best fits to the data, and differ from the predicted relations (gray curves).

Hulst's reddening curve No. 15 (see Johnson 1966). In addition, the observations for Hyades stars were supplemented by data from Carney (1982) in order to reduce the photometric scatter typical of 2MASS observations. The results are plotted in the lower panel of Figure 1.

The observational trends of $V–J$, $V–H$, and $V–K_s$ are fairly similar to the predicted trends seen in the upper panel of Figure 1, but with noticeable offsets, particularly in $V–H$. The adopted intrinsic relations were therefore established from polynomial fits to the observational data rather than from the predicted relations, with the results tabulated in Table 1 for zero-age main sequence (ZAMS) stars. The derived polynomial relationships of Figure 1 were used to derive intrinsic $J–H$ and $H–K$ colors for main-sequence stars as a function of intrinsic broad band color index $(B–V)_0$, and the ZAMS calibration was that of Turner (1976b, 1979).

The intrinsic relationship for 2MASS colors in Table 1 is similar to the intrinsic color-color relation for dwarf stars in the UBV system, displaying a noticeable "kink" near spectral type A0. 2MASS J magnitudes sample the Brackett continuum in hot stars, while H and K_s magnitudes sample the Pfund continuum, so $J–H$ color should provide a measure of the Pfund discontinuity in hot stars, much like $U–B$ color provides a measure of the Balmer discontinuity. Similarly, $H–K_s$ color should provide a measure of stellar temperature, much like $B–V$ color does in the UBV system. For cool stars all colors should closely track changes in the slope of the black body continuum in the far infrared. Interstellar reddening affects JHK_s colors much less than it does UBV colors, but the effects of circumstellar emission are often more important in the far infrared than in the visible region. A UBV color-color diagram plots $U–B$ versus $B–V$, for which a plot of $J–H$ versus $H–K_s$ would be the closest approximation. It appears, however, that $J–H$ colors may display a greater precision than $H–K_s$ colors in 2MASS photometry, so the diagnostic tool used here to establish reddening for cluster stars is a 2MASS color-color diagram in which $H–K_s$ is plotted versus $J–H$.

The intrinsic relations were tested further using the three clusters used for the calibration and three additional clusters that lie in fields of uniform interstellar reddening: Stock 16 (Turner 1985a), NGC 2362 (Johnson & Morgan 1953; Johnson 1957; Johnson et al. 1961), and NGC 2281 (Pesch 1961), which are reddened by $E(B–V) = 0.49$, 0.11, and 0.11, respectively (see Turner 1996; Johnson et al. 1961). Obvious unreddened stars in the same fields were also included in the samples. Figure 2 plots 2MASS colors for stars in the core regions of Stock 16, NGC 2362, and NGC 2281 with cited magnitude uncertainties of less than ± 0.05, corrected for their known reddening or lack of reddening for suspected foreground stars, along with similar data for Hyades and Ursa Major cluster stars and dereddened data for stars in NGC 2244. Data for the Ursa Major cluster include 11 stars with observations of uncertain quality (bright stars with saturated photometry and blended stars). The lower right portion of Figure 2 displays the data for all clusters, except for UMa stars of poor quality, combined using running 20-point means as a function of $J–H$ color. The last step was made as a means of reducing the photometric scatter in both colors.

The intrinsic relation of Table 1 appears to be confirmed by stars in the open clusters of Figure 2, although there is clearly additional scatter in the observations of individual stars that cannot be attributed to differential reddening. In three of the